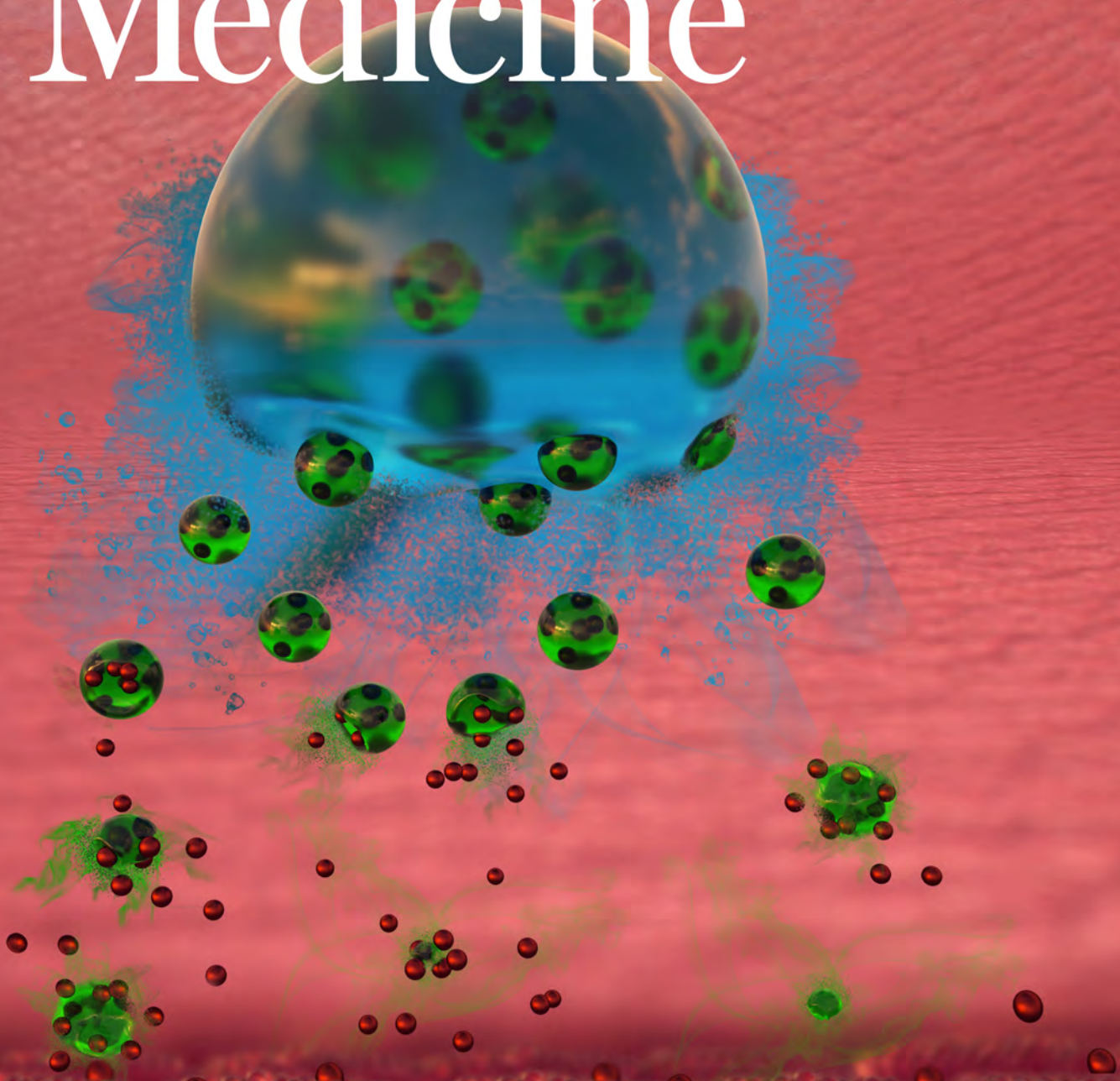# Science Translational Medicine

DRUG DELIVERY

A heat-stable microparticle platform for oral micronutrient delivery

Aaron C. Anselmo[1]*[†], Xian Xu[1]*, Simone Buerkli[2]*, Yingying Zeng[1], Wen Tang[1],
Kevin J. McHugh[1][‡], Adam M. Behrens[1], Evan Rosenberg[1], Aranda R. Duan[1], James L. Sugarman[1],
Jia Zhuang[1], Joe Collins[1], Xueguang Lu[1], Tyler Graf[1], Stephany Y. Tzeng[1], Sviatlana Rose[1],
Sarah Acolatse[1], Thanh D. Nguyen[1][§], Xiao Le[1], Ana Sofia Guerra[3], Lisa E. Freed[1][‖],
Shelley B. Weinstock[4], Christopher B. Sears[5], Boris Nikolic[6], Lowell Wood[7], Philip A. Welkhoff[7][¶],
James D. Oxley[8], Diego Moretti[2][#], Michael B. Zimmermann[2], Robert Langer[1]**, Ana Jaklenec[1]**

Micronutrient deficiencies affect up to 2 billion people and are the leading cause of cognitive and physical disorders in the developing world. Food fortification is effective in treating micronutrient deficiencies; however, its global implementation has been limited by technical challenges in maintaining micronutrient stability during cooking and storage. We hypothesized that polymer-based encapsulation could address this and facilitate micronutrient absorption. We identified poly(butylmethacrylate-co-(2-dimethylaminoethyl)methacrylate-co-methylmethacrylate) (1:2:1) (BMC) as a material with proven safety, offering stability in boiling water, rapid dissolution in gastric acid, and the ability to encapsulate distinct micronutrients. We encapsulated 11 micronutrients (iron; iodine; zinc; and vitamins A, B2, niacin, biotin, folic acid, B12, C, and D) and co-encapsulated up to 4 micronutrients. Encapsulation improved micronutrient stability against heat, light, moisture, and oxidation. Rodent studies confirmed rapid micronutrient release in the stomach and intestinal absorption. Bioavailability of iron from microparticles, compared to free iron, was lower in an initial human study. An organotypic human intestinal model revealed that increased iron loading and decreased polymer content would improve absorption. Using process development approaches capable of kilogram-scale synthesis, we increased iron loading more than 30-fold. Scaled batches tested in a follow-up human study exhibited up to 89% relative iron bioavailability compared to free iron. Collectively, these studies describe a broad approach for clinical translation of a heat-stable ingestible micronutrient delivery platform with the potential to improve micronutrient deficiency in the developing world. These approaches could potentially be applied toward clinical translation of other materials, such as natural polymers, for encapsulation and oral delivery of micronutrients.

INTRODUCTION

Micronutrient deficiencies are prevalent across the developing world, affecting 2 billion people (1) and causing cognitive and physical disorders such as anemia, blindness, birth defects, impaired growth in children (2–7), and around 2 million childhood deaths per year (8–10). Large-scale human trials have established that micronutrient fortification of foods can effectively treat micronutrient deficiencies (11–18), but this approach has been limited (19–21) because of poor implementation in certain countries and unaddressed technical challenges related to micronutrient stability during storage and cooking. For example, heat, moisture, and oxidation encountered during cooking can impair absorption of vitamins through degradation (17, 18, 22–26) or make food unpalatable through chemical changes to minerals (27). Hence, the development of technologies that address these stability challenges can facilitate implementation of staple food fortification and affect global health by treating worldwide micronutrient deficiencies.

Current micronutrient technologies focus on encapsulation in microparticles (MPs), nanoparticles, agglomerates, and powders using biopolymers and food additives such as proteins, polysaccharides, lipids, and surfactants (28–33). However, these approaches are limited in addressing the stability challenges encountered during end use of the micronutrients (cooking) and delivery challenges related to micronutrient release and subsequent absorption by the body. We hypothesized that we could address this by using a pH-sensitive polymer that encapsulates both water-soluble and fat-soluble micronutrients; protects the encapsulated micronutrient from high temperature, moisture, and oxidizing agents; and rapidly releases in the stomach to ensure intestinal absorption.

Using an encapsulating matrix, we describe an MP delivery platform that encapsulates 11 micronutrients individually and up to 4 micronutrients in combination; enhances micronutrient stability after exposure to boiling water, light, or oxidizing chemicals found in common foods; and rapidly releases micronutrients upon exposure

[1]David H. Koch Institute for Integrative Cancer Research, Massachusetts Institute of Technology, Cambridge, MA 02139, USA. [2]Institute of Food Nutrition and Health, ETH Zürich, Zürich 8092, Switzerland. [3]Department of Chemistry and Chemical Biology, Harvard University, Cambridge, MA 02138, USA. [4]Institute of Human Nutrition, Columbia University College of Physicians and Surgeons, New York, NY 10032, USA. [5]Independent Scholar, Belmont, MA 02478, USA. [6]Biomatics Capital, 1107 1st Avenue, Apartment 1305, Seattle, WA 98101, USA. [7]Institute for Disease Modeling, Bellevue, WA 98005, USA. [8]Southwest Research Institute, San Antonio, TX 78238, USA.
*These authors contributed equally to this work.
†Present address: Division of Pharmacoengineering and Molecular Pharmaceutics, Eshelman School of Pharmacy, University of North Carolina at Chapel Hill, Chapel Hill, NC 27599, USA.
‡Present address: Department of Bioengineering, Rice University, Houston, TX 77030, USA.
§Present address: Department of Mechanical Engineering, University of Connecticut, Storrs, CT 06269, USA.
‖Present address: Media Lab, Massachusetts Institute of Technology, Cambridge, MA 02139, USA.
¶Present address: The Bill & Melinda Gates Foundation, Seattle, WA 98109, USA.
#Present address: Nutrition Group, Health Department, Swiss Distance University of Applied Sciences, Regensdorf CH-8105, Switzerland.
**Corresponding author. Email: jaklenec@mit.edu (A.J.); rlanger@mit.edu (R.L.)

Anselmo et al., Sci. Transl. Med. 11, eaaw3680 (2019) 13 November 2019

1 of 13

to simulated gastric fluid (SGF). In vivo studies confirmed rapid micronutrient release in the stomach and subsequent absorption in the small intestine. In humans, we investigated the bioavailability of ferrous sulfate (iron) after ingestion of iron-loaded MPs. Alongside complementary studies in an organotypic intestinal model, we identified MP iron loading and MP polymer content to be absorption-limiting parameters in humans. We then developed and subsequently leveraged large-scale process development approaches to simultaneously increase loading and decrease polymer content in MPs. In a second human trial, MPs synthesized at scale with higher iron loading and lower polymer content demonstrated non-inferior absorption as compared to non-MP controls. These results indicate that this MP platform can be used to individually encapsulate or co-encapsulate micronutrients in a modular manner, maintain stability over 2 hours in boiling water, and then rapidly release in gastric conditions to successfully deliver micronutrients to humans. Overall, our study details a broad approach from conception to human trials of a highly heat-stable MP platform for oral micronutrient delivery.

RESULTS

Formulation of MPs at laboratory scale

We initially considered more than 50 potential polymers that could simultaneously be stable in boiling water and dissolve rapidly in low pH and closely evaluated 10 candidates (table S1). BMC [poly(butylmethacrylate-co-(2-dimethylaminoethyl)methacrylate-co-methylmethacrylate) (1:2:1)], available commercially as either a U.S. Food and Drug Administration (FDA)–approved inactive ingredient (Eudragit E PO powder) or a self-affirmed generally recognized as safe (GRAS) status material (Eudraguard Protect powder), was selected as the MP encapsulation material as it simultaneously addresses the above challenges (table S1) (34–41). Micronutrients were encapsulated individually in MPs using a one-step (Fig. 1A) or two-step (Fig. 1B) emulsion process, followed by centrifugation to remove unencapsulated micronutrients. In both approaches, BMC was used as the encapsulant; however, the two-step process used either hyaluronic acid (HA) or gelatin as an additional stabilizing excipient included in the first step (Fig. 1B). For the two-step process, MPs sampled during the first step were about 5 μm in diameter (Fig. 1C), whereas after the second step, they exhibited a hierarchical particle-in-particle structure about 200 μm in diameter (Fig. 1, D and E). The two-step process was used for water-soluble micronutrients that could not be encapsulated using the one-step process due to non-homogeneous suspension of water-soluble micronutrients. This two-step approach was additionally used to enable the co-encapsulation of vitamins A, D, folic acid, and B12 (fig. S1). In contrast, MPs synthesized via the one-step process exhibited homogeneous internal structure and were about 200 μm in diameter (Fig. 1F). Formulation parameters, loadings, and encapsulation efficiencies for each of the laboratory-scale MPs are shown in table S2.

Controlled release of micronutrients in vitro

In vitro release studies confirmed the retention of micronutrients in the encapsulated MPs after exposure to room temperature (RT) water or boiling (100°C) water (Fig. 2). pH-responsive burst release was exhibited when particles were exposed to 37°C SGF at pH 1.5 (Fig. 2). Micronutrient retention during 2 hours in boiling water was used as a baseline index of MP stability under simulated cooking conditions, because micronutrients such as vitamin A undergo chemical degra-

dation when exposed to high temperature or humidity (16, 17). The one-step process was confirmed to achieve retention (>80% at 120 min) in 100°C or RT water and rapid release (>80% at 30 min) in 37°C SGF for most individually encapsulated micronutrients (Fig. 2). The two-step process was developed to further stabilize highly water-soluble micronutrients within the BMC matrix (Fig. 2). More specifically, when the two-step process that included HA as the stabilizing biopolymer was used to encapsulate $FeSO_4$, the payload was largely retained (>90% at 120 min) in 100°C or RT water and rapidly released (>80% at 30 min) in 37°C SGF, whereas $FeSO_4$ formulations synthesized via the one-step process exhibited payload release even in RT water. The role of pH in modulating release kinetics was investigated using vitamin B12 as a representative micronutrient, where payload release was achieved more rapidly at lower pH values (fig. S2). Time-lapse imaging of vitamin A–BMC MPs immersed in SGF exhibited payload release in <1 min (Fig. 2B), as did Fe-HA-BMC MPs (Fig. 2C). Four co-encapsulated vitamins, water-soluble vitamins B12 and folic acid introduced in step 1 and fat-soluble vitamins A and D introduced in step 2 (fig. S1), each maintained payload retention (>80% at 120 min) in 100°C or RT water and rapidly released (60 to 90% at 30 min) the payloads in 37°C SGF (Fig. 2, D to G). Together, these results indicate that the BMC MP platform system can be used to individually encapsulate or co-encapsulate micronutrients in a modular manner, provide retention during 2 hours in boiling water, and enable burst release in 37°C SGF.

Micronutrient stability under heat, water, ultraviolet light, and oxidizing agents

Many micronutrients, such as vitamin A (23–25) and iron (26), are sensitive to high temperatures, moisture, ultraviolet (UV) light, or oxidizing chemicals, which can lead to degradation or changes in the oxidative states and thus limit absorption after ingestion (26). Hence, we studied the role that BMC encapsulation plays in improving micronutrient stability against these challenges for both individually and co-encapsulated formulations. We first investigated protection of the micronutrient payload during 2 hours in boiling water, which exposed the payload to high temperatures and moisture. For the encapsulated fat-soluble micronutrients vitamin A and D, more than 5- and 18-fold enhanced recovery was observed, respectively, as compared to unencapsulated counterparts (Fig. 3A), after exposure to boiling water conditions for 2 hours. Similarly, encapsulation protected water-soluble vitamins C and B2 during boiling, as both water-soluble vitamin groups exhibited enhanced recovery as compared to unencapsulated controls (Fig. 3A). We next investigated protection of the micronutrient payload after 24 hours of light exposure (280 μW/cm^2), because both vitamin A (32) and vitamin D (42) are rapidly degraded by UV light in their unencapsulated forms (Fig. 3B). Recovery after light exposure was significantly improved by more than 15- and 3-fold for vitamin A and D, respectively, encapsulated in BMC MPs as compared to unencapsulated controls ($P < 0.05$; Fig. 3B).

Similar to individually encapsulated micronutrients, co-encapsulated micronutrients maintained their biological activity after exposure to boiling water for up to 2 hours (Fig. 3C). Negative oxidizing interactions between micronutrients in fortified products and micronutrients naturally present in food sources readily occur, and these interactions can negatively affect absorption and bioavailability (18). For example, polyphenols present in food catalyze iron oxidation, resulting in a marked color change, from a highly bioavailable ferrous
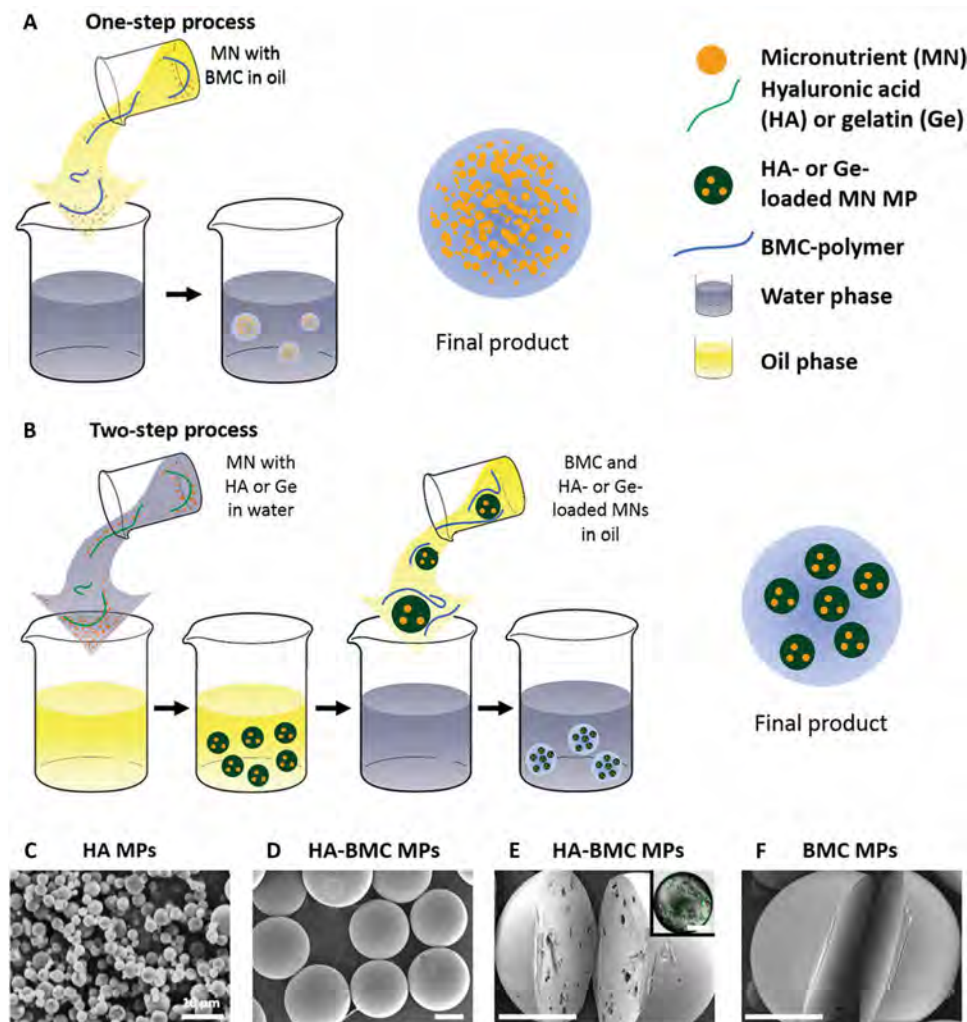
Fig. 1. Particle synthesis and characterization. Schematic representations of the (**A**) one-step and (**B**) two-step processes for formulating MPs. SEM images of (**C**) HA MPs, (**D**) HA-BMC MPs, (**E**) the cross section of an HA-BMC MP (inset, confocal image of an HA-BMC MP with fluorescently labeled HA), and (**F**) the cross section of a BMC MP. Scale bars, 100 μm, unless otherwise noted.

Release of a model payload and absorption of vitamin A in vivo

To confirm BMC MP dissolution in vivo, we used female SKH1-Elite mice to track payload release using the near-infrared fluorescent dye 1,1′-dioctadecyl-3,3,3′,3′-tetramethylindotricarbocyanine iodide (DiR) encapsulated in BMC. DiR can be differentiated in the encapsulated and released states by investigating the influence of environmental conditions on DiR's fluorescent properties using established imaging techniques (*44*). A 14-point spectral fingerprint of a DiR-loaded BMC MP was obtained when the MP was suspended in water. In contrast, when DiR is released from a BMC MP in SGF, the resulting blue shift exhibits a spectral profile distinct from encapsulated DiR. Hence, the encapsulated and released DiR could be differentiated using their distinct fluorescent fingerprints (fig. S4). The two fingerprints of the dye in either encapsulated or released form were used to indirectly reflect the dissolution of the BMC MPs in vivo. DiR-loaded BMC MPs were administered orally to mice, and at timed intervals, the animals were euthanized and the complete gastrointestinal tract was excised for ex vivo fluorescence imaging (Fig. 4A). Both the physical state of the dye (encapsulated or released) and the physiological location of the dye in the gastrointestinal tract were visualized (Fig. 4A) and quantified (Fig. 4B). At 15 min, the stomach contained a mixture of encapsulated and released DiR, suggesting that the BMC MPs were partially dissolved and a portion of payload was released but had not yet entered the intestines. At 30 min, DiR signal was predominantly detected as both encapsulated dye in the stomach and released dye in the intestines. At 60 min, minimal signal of BMC-encapsulated DiR was detectable, highlighting how the majority of particles released their payload within 1 hour. Furthermore, at 1 hour, the released dye signal was exclusively in the intestines, implying that the released payload had passed through the stomach and into the intestines within 1 hour. These findings confirm rapid release of a model payload from orally administered MP into the murine gastrointestinal tract. To determine whether this rapid release would facilitate absorption of encapsulated micronutrients, we evaluated the absorption of vitamin A in female Wistar rats. Tritium-labeled vitamin A was orally administrated to rats by gavage in both the free form and BMC-encapsulated forms, and blood samples were taken to evaluate vitamin A content over a period of 6 hours (Fig. 4C). Encapsulated vitamin A exhibited statistically indistinguishable absorption relative to free vitamin A (Fig. 4C), highlighting that encapsulation in BMC did not influence absorption.
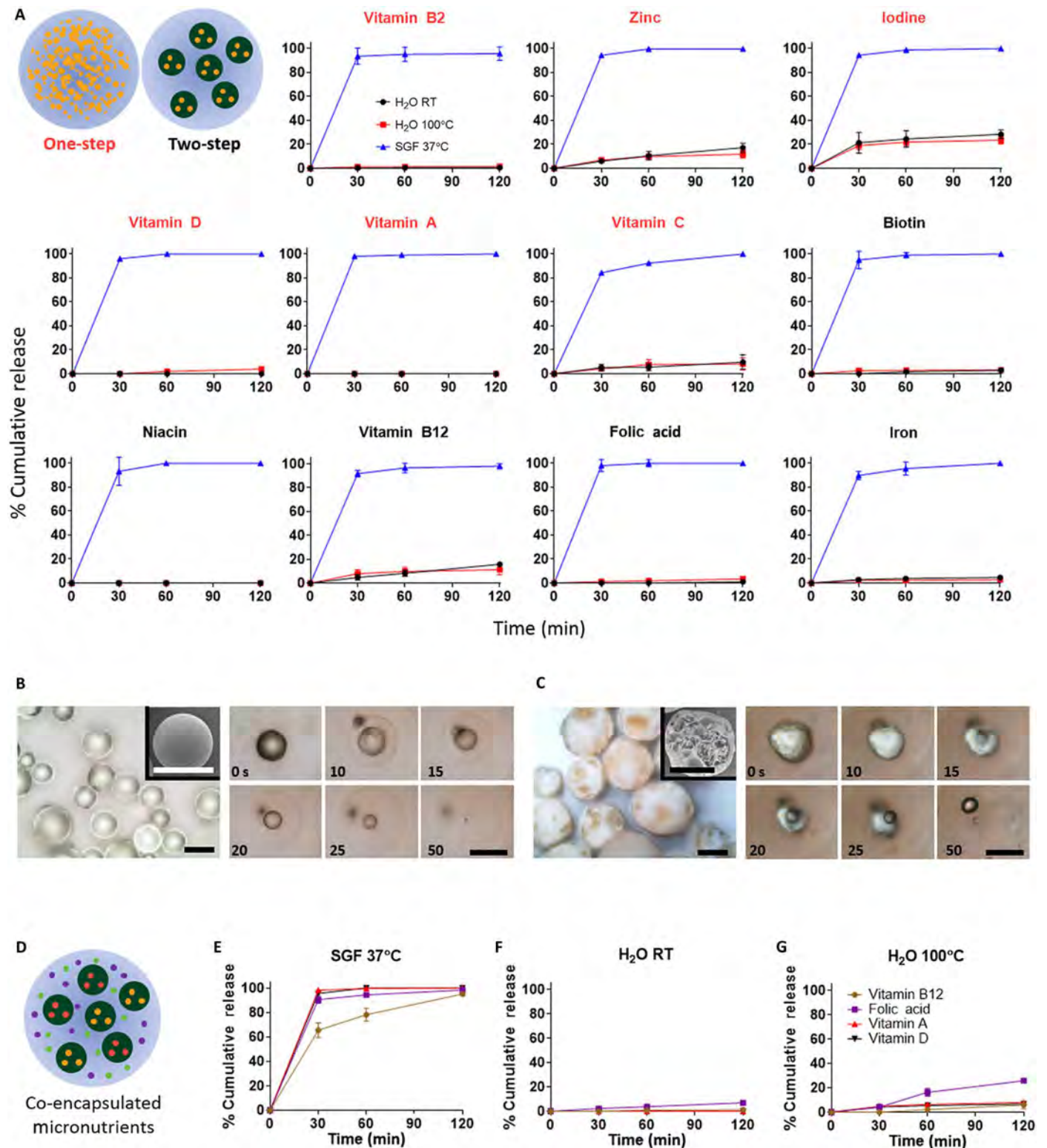
(Fe^{2+}) state to a ferric state (Fe^{3+}) (*43*) that exhibits poor bioavailability (*26*). To examine whether BMC encapsulation prevents interactions between the encapsulated iron and oxidizing chemicals present in food, BMC-encapsulated and unencapsulated iron was added to polyphenol-rich banana milk and the color change was quantified over time. Iron encapsulation in HA-BMC MPs exhibited less color change, and therefore less oxidation, in banana milk as compared to unencapsulated iron (Fig. 3D). These results indicate that the BMC MP matrix can limit interactions between the encapsulated iron and the free polyphenols in food. Last, to demonstrate a maintained capability for pH-controlled release of iron after exposure to high temperature, moisture, and oxygen, iron-loaded MPs that were first boiled for 2 hours and then immersed in SGF were visualized using real-time microscopy, confirming that they maintained their ability to rapidly release their iron payload at low pH (Fig. 3E). After boiling, HA-BMC MPs retained similar morphology (fig. S3) to pre-boiling (Fig. 1D). Overall, these results indicate that encapsulation in BMC protects micronutrient payloads during exposure to high temperatures, moisture, UV light, and oxidizing chemicals.

Fig. 2. Controlled release of micronutrients. (**A**) Percent cumulative release of 11 different individually encapsulated micronutrients in 37°C SGF, pH 1.5 (blue lines), and RT water (black lines) or boiling water (red lines). Schematic shows micronutrients encapsulated via one-step process (red text) versus two-step process (black text). (**B** and **C**) Representative bright-field images and time-lapse release of (B) vitamin A from BMC MPs and (C) iron from HA-BMC MPs in SGF (insets, SEMs). (**D**) Schematic of four co-encapsulated micronutrients [folic acid (purple), B12 (brown), vitamin A (red), and vitamin D (black)] and percent cumulative release in (**E**) 37°C SGF, (**F**) RT water, and (**G**) boiling water. Error bars represent SD of the mean (*n* = 3). Scale bars, 200 μm.
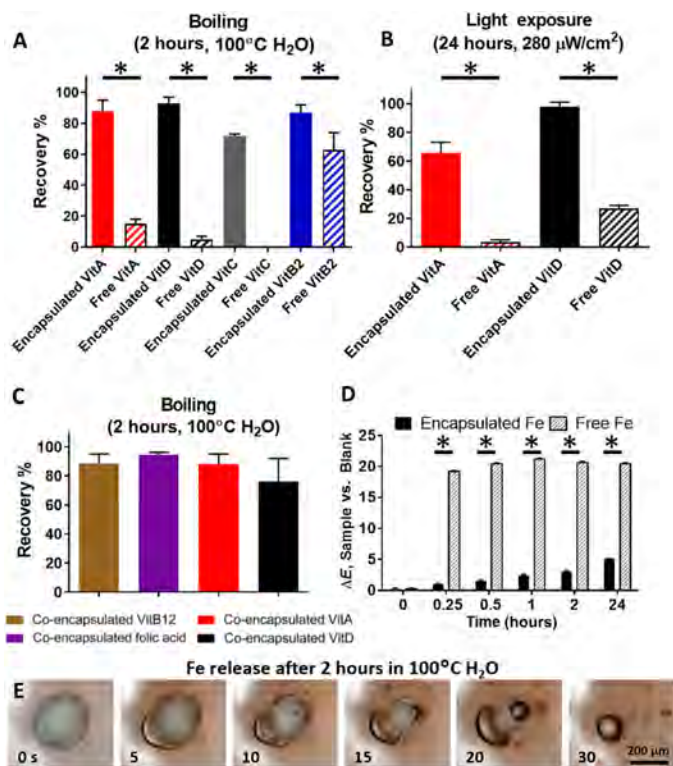
Fig. 3. Protection from heat, light, and chemical interactions. Recovery of individually encapsulated versus unencapsulated (free) micronutrients after exposure to (**A**) boiling water and (**B**) light. (**C**) Recovery of co-encapsulated micronutrients after boiling in water. (**D**) Time history of color change (ΔE), an indication of a chemical reaction between iron and polyphenols present in banana milk, of laboratory-scale Fe-HA-BMC MPs versus unencapsulated (free) iron. (**E**) Time-lapse release of iron from HA-BMC MPs after boiling in water for 2 hours at RT and upon immersion in RT SGF. Error bars represent SD of the mean ($n = 3$). *$P < 0.05$ as determined by Student's t test.

Bioavailability of iron in humans and iron transport in an in vitro intestinal barrier model

Fe-HA-BMC MPs were investigated for their ability to deliver bioavailable iron in humans. Iron bioavailability was investigated through the consumption of three stable iron isotope–labeled test meals administered in a randomized single-blind, cross-over design to fasting young women {$n = 20$; mean ± SD, hemoglobin (Hb) = 13.4 ± 0.85 g/liter; and geometric mean [95% confidence interval (CI)], plasma ferritin (PF), 11.6 (9.4, 14.5) μg/liter} (table S3). The test meals were whole-grain maize porridge with vegetable sauce, an iron absorption inhibitory meal (45) with an iron:phytic acid molar ratio of 1:6.5 and negligible (0.4 mg/meal) ascorbic acid content, to which labeled unencapsulated or encapsulated ferrous sulfate was added after cooking. Two test meals contained 4 mg of iron as labeled ferrous sulfate (either ^{54}Fe or ^{57}Fe) in HA-BMC MPs (encapsulated iron), which was added either before or after cooking, to investigate the effects that cooking (30 min of baking at 100°C) had on iron bioavailability after MP encapsulation. The third test meal, the reference, contained 4 mg of unencapsulated iron (free) as labeled ferrous sulfate (^{58}Fe). The geometric mean (95% CI) of fractional iron absorption (FIA) of the reference meal (free uncooked Fe) was 3.36 (2.29, 4.95)%, whereas the FIA of ferrous sulfate from uncooked Fe-HA-BMC MPs was 1.46 (0.77, 2.79)% (Fig. 5A). Fe-HA-BMC MPs exhibited 44

(22, 88)% relative iron bioavailability (RBV) as compared to unencapsulated ferrous sulfate ($P < 0.01$) (Fig. 5A). Cooking the encapsulated ferrous sulfate had no effect on its bioavailability [FIA, 1.41 (0.91, 2.19)%; RBV, 42 (34, 53)%] (Fig. 5A).

Although the first human study showed that Fe encapsulation in HA-BMC MPs reduces iron bioavailability as compared to unencapsulated iron (Fig. 5A), our platform demonstrated efficacy in delivering bioavailable iron to humans, independent of cooking conditions (Fig. 5A). It has been previously reported that materials that encapsulate micronutrients can interfere with absorption (15); hence, we investigated the role that HA and BMC independently play in the intestinal absorption of iron. In vitro studies were designed to simulate conditions of iron penetration of the intestinal epithelial cell barrier in humans after oral ingestion of Fe-HA-BMC MPs. A commercially available human intestinal epithelial cell barrier model (EpiIntestinal, MatTek) provided a test platform to investigate the effect the MP constituents have on intestinal iron absorption by systematically varying the relative concentrations of iron, HA, and BMC. The model consisted of primary small intestine epithelial cells obtained from a healthy human donor, dissociated enzymatically, and cultured in customized medium on cell culture inserts within 12-well plates to form a functional, columnar-like three-dimensional epithelial barrier layer (46).

Oral administration of iron formulations was modeled by adding samples into the apical surface of the intestinal barrier, accessible as the cell culture insert in the upper compartment of the well plate, and, after a 1-hour incubation period, quantifying iron transport as the amount that passed through the tissue barrier and could be determined by analysis of the culture medium in the lower compartment of the well plate. The transport of iron added in combination with HA (Fig. 5B) and/or BMC (Fig. 5C) was expressed as a percentage of the transport of free iron added in the absence of HA or BMC. HA presence exhibited no significant effect on iron transport through the intestinal barrier (Fig. 5B). Moreover, iron was readily transported through the barrier at the Fe:HA ratio used in the MPs tested in this first human study. In contrast, unencapsulated BMC added to iron at increasing percentages significantly reduced iron transport through the intestinal barrier (Fig. 5C). In particular, iron was poorly transported through the barrier when present at the BMC percentage of 96%, which corresponds to the percent BMC in the MPs tested in human subjects. At the percentage of BMC present in the current MP formulation, iron transport was reduced to 37% compared to free iron. Similarly, iron transport was reduced to 33% of that measured for free iron when the neutralized contents of MPs dissociated by incubation in SGF were added to the intestinal barrier (Fig. 5C). As BMC percentage decreased, the iron transport–inhibiting effects of BMC became negligible, which indicates that formulations containing lower percentage of BMC may not inhibit iron transport across the intestines. By using this organotypic model to determine the conditions that do not inhibit iron transport, we have highlighted the utility of in vitro models for use in screening micronutrient formulations to inform MP design (47).

Process development and scale-up

The MPs described were conceived and synthesized as laboratory-scale research formulations. Although emulsion-based microencapsulation methods are a staple in many biomaterial and formulation laboratories at the academic level (28, 48), we encountered considerable challenges in increasing the iron loading when encapsulated in
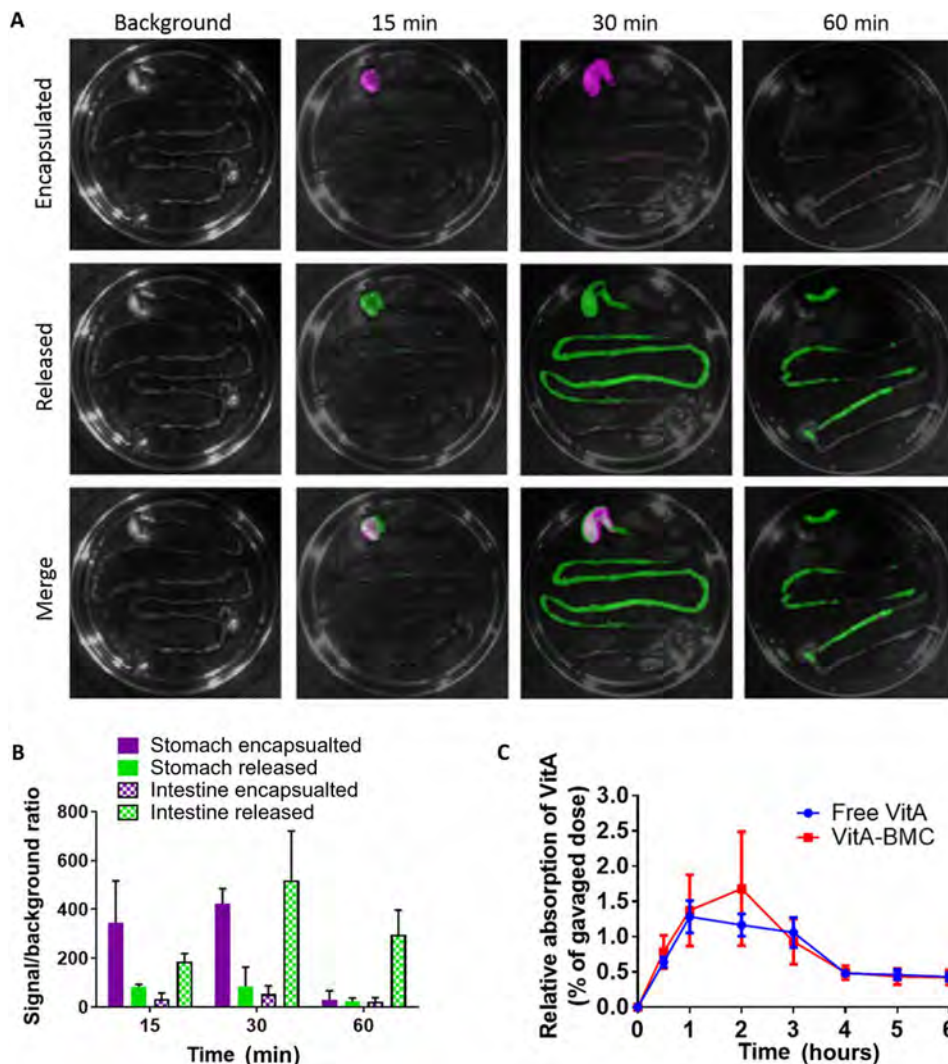
Fig. 4. In vivo release of a model dye and absorption of vitamin A. (**A**) Representative IVIS images (logarithmic scale) of explanted murine gastrointestinal tract harvested after oral administration of dye-loaded BMC MPs showing encapsulated dye (purple) and released dye (green) over 60 min. (**B**) Quantitative analysis of encapsulated dye in the stomach (solid purple bars), released dye in the stomach (solid green bars), encapsulated dye in the intestines (hatched purple bars), and released dye in the intestines (hatched green bars). Error bars represent SD of the mean (*n* = 3). (**C**) Blood content of radiolabeled vitamin A over a 6-hour period after oral gavage of free vitamin A (blue lines) or VitA-BMC MPs (red lines). Error bars represent SEM (*n* = 6).

iron in SGF in less than 5 min (fig. S5C). As expected, the release of iron in pH 5 buffered water demonstrated a pH dependency (fig. S5, A and B). For human studies, food-grade iron-loaded BMC particles with acceptable values for residual dichloromethane (DCM), endotoxins, and microbial bioburden (table S5) were used. These scaled MPs were also examined for their ability to prevent interactions between the encapsulated iron and oxidizing chemicals present in food as described above with polyphenol-rich banana milk. It was demonstrated that the scaled Fe-HA-BMC MPs induced less color change as compared to all free forms of iron, both with and without the other MP constituents (HA, BMC, and HA with BMC) (fig. S5D).

Bioavailability of iron particles of 5- and 30-fold higher loading in humans

Fe-HA-BMC MPs at more than 5-fold and more than 30-fold higher iron loading, compared to the laboratory-scale batch used in the first human trial, were investigated for their ability to deliver bioavailable iron to humans in a second human study. In this study, a non–iron-inhibiting food matrix (wheat bread) was used to better compare unencapsulated iron and encapsulated iron by solely focusing on absorption, as opposed to both absorption and particle-mediated protection against small molecules that chelate iron. Nine test meals containing identical doses of iron (4 mg Fe) were administered in a partially randomized single-blind, crossover design to fasting young women [*n* = 24; Hb, 13.2 ± 0.95 g/liter; and PF, 13.2 (10.5, 16.5) µg/liter] (table S3). Three meals contained iron as labeled ferrous sulfate in 3.19% [54]Fe-HA-BMC MPs, 18.29% [57]Fe-HA-BMC MPs, and 4 mg of unencapsulated ferrous sulfate ([58]Fe, reference meal). In all cases, iron was added before baking the bread at 190°C for 20 min. In contrast to the first human study, 18.29% Fe-HA-BMC-MPs [FIA: 17.0 (13.2, 21.9)%] exhibited iron absorption that was not statistically different relative to unencapsulated iron [FIA: 19.2 (15.3, 24.29)%] (Fig. 7). The fivefold higher loaded 3.19% Fe-HA-BMC MPs [FIA: 13.7 (11.1, 16.8)%] exhibited significant lower absorption as compared to both unencapsulated and the highest loaded 18.29% Fe-HA-BMC MPs. Compared to the reference meal, 3.19 and 18.29% Fe-HA-BMC MPs exhibited 71 (62, 82)% and 89 (74, 107)% RBV, respectively.

In this same human study, we investigated how competitive absorption, related to the co-delivery of other micronutrients or BMC-encapsulated micronutrients alongside Fe-HA-BMC MPs, can influence absorption of iron from Fe-HA-BMC MPs. Co-delivery
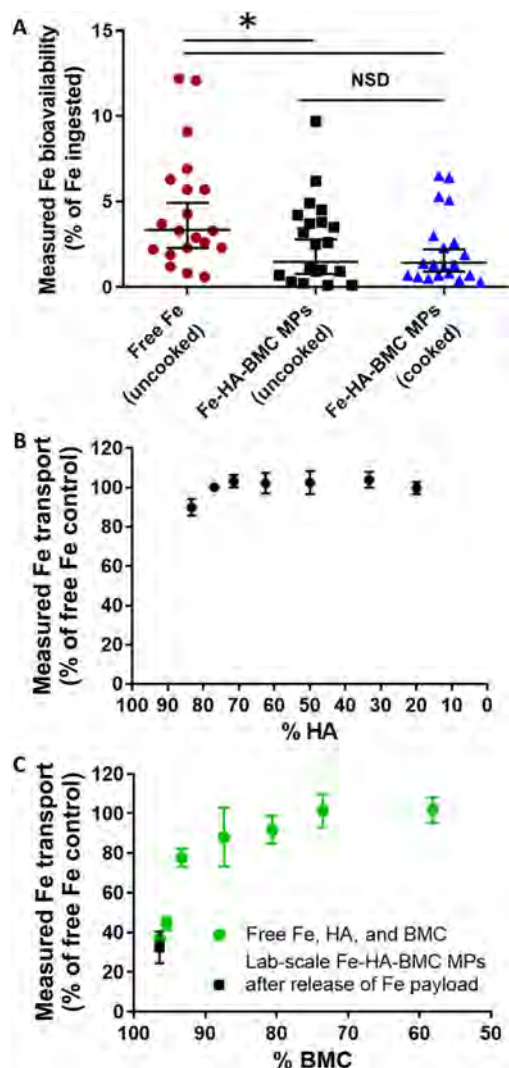
BMC. To address this, and to overcome the absorption issues that were encountered in the first human study, we developed new processes to increase the loading of iron in our formulation (Fig. 6A). A commercially available spray dryer and a customized spinning disc atomizer were used to formulate Fe-HA MPs (Fig. 6B) and Fe-HA-BMC MPs (Fig. 6C), respectively, at the kilogram scale. The initial scaled formulation was designed to recreate the 0.6% iron loading used in the first human study. Batches of Fe-HA-BMC MPs produced at the pilot scale (>1 kg) and at the same compositions of those used in the first human study met the same loading, stability, and pH-controlled release criteria as the laboratory-scale formulation tested in humans (Fig. 6D). We further developed processes to increase the loading of iron in BMC particles to 3.19% (fig. S5A) and 18.29% (fig. S5B), which additionally decreased BMC amounts (table S4). These scaled and high loaded iron BMC MPs exhibited near-complete release of

Anselmo *et al.*, *Sci. Transl. Med.* **11**, eaaw3680 (2019)   13 November 2019

6 of 13

Fig. 5. Bioavailability of iron in humans and iron transport in an in vitro intestinal barrier model. (**A**) Iron bioavailability as assessed by erythrocyte iron incorporation in young women ($n = 20$) after ingestion of unencapsulated (free) uncooked iron as $FeSO_4$ (red circles), encapsulated uncooked iron (black squares), and encapsulated cooked iron (blue triangles) and expressed as a percentage of the total amount that was ingested. Iron transported across a human in vitro intestinal barrier model after addition of iron in the presence of varying amounts of MP constituents (**B**) HA and (**C**) BMC and expressed as a percentage of transported free iron. Error bars in (A) represent geometric means ($n = 20$) with 95% CI. *$P < 0.05$, free Fe and each encapsulated group as determined by post hoc paired Student's t test with Bonferroni correction. Error bars in (B) and (C) represent SD of the mean ($n = 3$). NSD, no significant difference.

of VitA-BMC MPs [FIA: 12.7 (9.29, 17.5)%] or VitA-BMC MPs with free folic acid [FIA: 14.3 (11.2, 18.3)%] did not affect iron absorption (fig. S6), indicating that competition between co-delivered micronutrients or BMC-encapsulated micronutrients is not a major concern for the combinations studied here. In four additional test meals, we investigated the individual role of each MP component and how co-administering these components in free form influences absorption of iron as compared to formulation Fe-HA-BMC MPs. Our results indicated that absorption from free ferrous sulfate was not significantly affected by either HA [FIA: 20.7 (16.1, 26.7)%],

BMC [FIA: 16.6 (12.0, 23.2)%], or HA-BMC [FIA: 16.3 (11.7, 22.8)%]. Similarly, when Fe was encapsulated in HA [FIA: 15.1 (11.3, 20.3)%], iron absorption was not significantly different from the reference meal. Our results indicated that absorption was not significantly affected by either HA or BMC as compared to free iron; however, when HA and BMC were formulated as MPs, a decrease in absorption compared to free iron and free iron with HA was observed (fig. S7). This phenomenon is unlikely to occur for our highest loaded 18.29% Fe-HA-BMC MPs formulation, because it demonstrated comparable absorption relative to the reference (Fig. 7). Collectively, these results indicate that the absorption-limiting encapsulation that was observed in the first human study can be overcome and addressed through further development and increased loading of iron and decreased BMC content in HA-BMC MPs.

DISCUSSION

In this work, we describe polymer-based MPs that encapsulate 11 micronutrients individually or up to 4 in combination, maintain micronutrient stability during cooking and storage, and rapidly release micronutrient payloads. Modularity of the MP platform affords freedom to control the delivery and thus the dosing of each micronutrient for individual or large-population fortification needs. Studies in mice confirmed rapid micronutrient release in the stomach and absorption of vitamin A. In the first human study, the bioavailability of iron from iron-loaded MPs was verified to be 44% of unencapsulated iron control after oral ingestion. Using an organotypic human intestine model, we discovered that low iron loading and high BMC amount were responsible for the lower bioavailability in this first human study. Hence, process development approaches were leveraged to overcome these limitations of our laboratory-scale MPs. Industrially relevant spray drying and spinning disc atomization processes enabled increased iron loading while reducing the amount of BMC polymer in our iron-loaded MPs. In a subsequent human study, using iron-loaded BMC MPs of more than 5- and 30-fold higher iron loading and 25 and 85% less BMC polymer, we showed that our leading formulation exhibited statistically indistinguishable bioavailability as compared to an unencapsulated control. Specifically, the MP formulation of higher iron loading and lower BMC content used in the second human study address bioavailability issues; however, it should be noted that the highest iron-loaded MP exhibited lower stability in water and higher pH solutions. Hence, further optimization of BMC content and iron loading for both release and absorption may be required because variability of pH values in the stomach of human subjects at the time of ingestion (49) may be a potential source for observed absorption differences. Together, we describe a broad approach encompassing the design and clinical introduction of a controlled release platform for vitamins and minerals that can address unmet technological needs to improve global health. Furthermore, these approaches could readily be applied towards the clinical translation of other materials, such as natural polymers, for the encapsulation and oral delivery of micronutrients.

The basis of our strategy for food fortification focused on formulation of MPs using BMC, a polymer encapsulant that has historically been used for its advantages in encapsulation, enhancing stability, facilitating rapid and controlled release, toxicity, amenability to manufacturing processes, and widespread use in many nutraceuticals and pharmaceutical products (34–41, 50). BMC was selected after an in-depth analysis of more than 50 potential polymers. With regard to
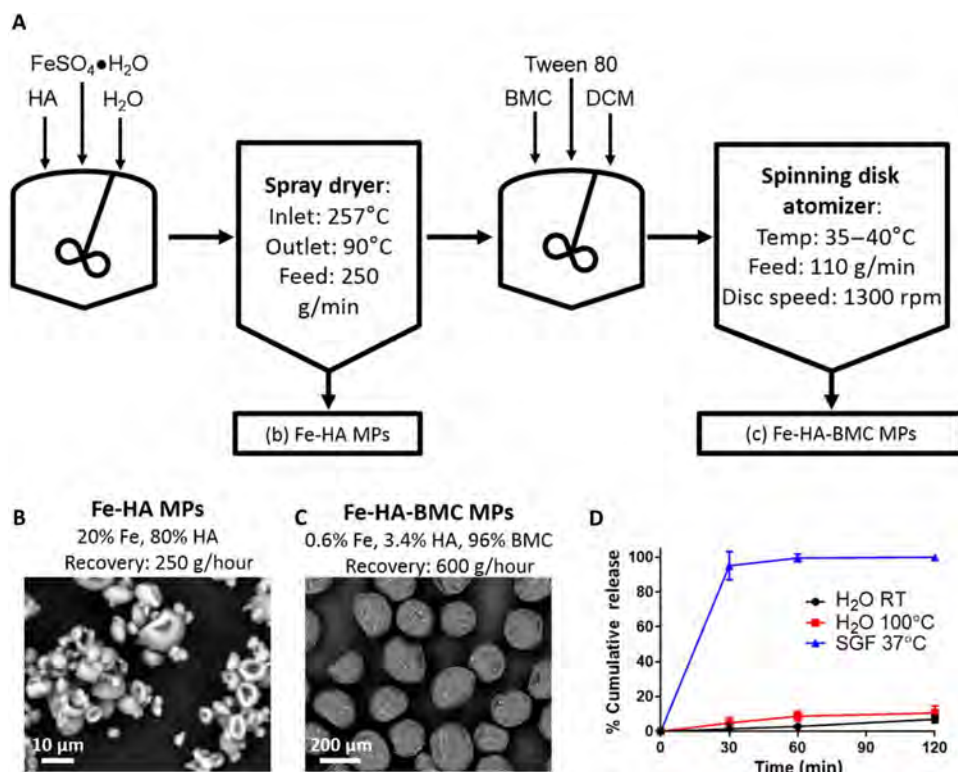
Fig. 6. Process development and scale-up. (**A**) Schematic showing the process for the scaled synthesis of 1 kg of Fe-HA-BMC MPs. SEM images of (**B**) the Fe-HA MP intermediate product and (**C**) the Fe-HA-BMC final product. (**D**) Iron release from scaled Fe-HA-BMC MPs in 37°C SGF, pH 1.5 (blue line), RT water (black line), and boiling water (red line). Error bars represent SD of the mean (n = 3).
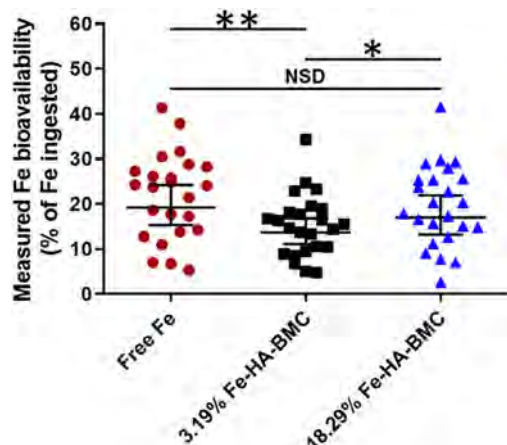

Fig. 7. Bioavailability of iron in humans from higher loaded Fe-HA-BMC MPs. Iron bioavailability as assessed by erythrocyte iron incorporation in young women (n = 24) after ingestion of free iron as FeSO₄ (red circles), 3.19% Fe-HA-BMC MPs (black squares), and 18.29% Fe-HA-BMC MPs (blue triangles) and expressed as a percentage of the total amount of iron that was ingested. Error bars represent geometric means (n = 24) and 95% CI. *P < 0.05 and **P < 0.01. Significant effect of meal on iron absorption determined by linear mixed models, participants as random intercept, meal as repeated fixed factor, and post hoc paired comparisons with Bonferroni correction P < 0.05.

enhanced stability, it has been previously demonstrated that the water vapor permeability of BMC (51) is lower than what is commonly used for preservation of fruits and vegetables (52); thus, it is

likely that the known moisture barrier properties of BMC provide protection against humidity and small-molecule diffusion by acting as a physical barrier between the payload and the environment. The UV-protective abilities of BMC can likely be attributed to the increased refractive index due to encapsulation in BMC (53), which will lower light exposure to encapsulated micronutrients. BMC is soluble at low pH in aqueous solutions and in non-aqueous solvents; hence, the solubility of BMC enabled rapid dissolution and release in stomach conditions, thus providing the versatility to facilitate encapsulation of 11 distinct micronutrients. An additional aspect of our reasoning for selecting BMC involves the existing infrastructure and knowledge base that would enable the translation of a BMC-based technology. For example, BMC is already used commercially, has been shown to be compatible with large-scale manufacturing processes, has a history of acceptance by the FDA, and is generally regarded as safe (54). The choice of solvent, DCM, used in the particle fabrication process at scale and removed afterward, has essential roles in the preparation of other everyday consumer products such as decaffeinated coffee (55). Recently, the Joint Food and Agriculture Organization of the United Nations and the World Health Organization Expert Committee on Food Additives (JECFA) yielded a positive response for BMC, specifically for micronutrient encapsulation for food fortification (56). JECFA concluded that the use of BMC is not a safety concern when the food additive is used for micronutrient encapsulation for food fortification at the intended use amounts and recommended an acceptable daily intake of "not specified." Subsequently, the Codex Committee on Food Additives (CCFA) agreed to accept the JECFA recommendations (57). Hence, concerns about the toxicity of BMC have been previously and extensively evaluated and addressed (50, 54); furthermore, the doses described here and the potential doses that may be used in practice would be unlikely to exceed the well-published limitations for oral exposure.

The human absorption studies described here were performed in a well-controlled setting. Both studies were performed in young healthy women where the prevalence of iron deficiency in the study population was 65 and 58% in human studies 1 and 2, respectively. The meal was specified in terms of mass and volume, the dosing of encapsulated iron was measured precisely, and the cooking conditions were well controlled using standardized procedures. Iron status will likely differ in real-world settings where people consuming the micronutrients will be from different countries where staple foods vary. In addition, the age, health status, and eating habits of individuals will vary in different cultures as well as within households. Hence, further human testing for efficacy, especially in target countries and populations, will be informative for evaluating and developing these

Anselmo et al., Sci. Transl. Med. **11**, eaaw3680 (2019)   13 November 2019

8 of 13

micronutrient formulations to ensure that they are suitable in terms of stability, release, and absorption. In previous work, it has been shown that the encapsulating material can inhibit iron bioavailability (15, 18), which agrees with the results from both of our human studies. This relationship between the encapsulant and the micronutrient is directly tied to absorption and should be further studied for our MP platform in animals and in humans. Since micronutrients such as vitamin A or D are more sensitive to thermal degradation as compared to iron, there exists a unique opportunity to leverage our MP platform for the storage and delivery of highly sensitive micronutrients. Our preliminary storage and in vivo absorption work suggest that delivery of nonmineral micronutrients will be promising; however, further evidence is needed in humans. We also demonstrated successful co-encapsulation of vitamins A, D, folic acid, and B12; future efforts should focus on investigating how co-encapsulated micronutrients with known compatibility issues (58) may interact with each other, as this study was designed to evaluate bioavailability of a single micronutrient (iron). The experimental approaches we have detailed here lay the groundwork to facilitate these additional studies and provide a path toward clinical translation.

In practice, translation of this technology for worldwide use, especially in countries in need of solutions for nutrition deficiencies, will still require scaling beyond the kilogram batch size to metric tons. The spray drying and atomization processes described here are translatable to current commercial scale processes for micronutrients (59). Hence, the main cost implication is directly related to the added raw material cost of BMC; future considerations to offset this cost or justify it must be considered on a country or regional level, because the severity of micronutrient deficiencies will be a driving force to balance the technical advantages offered by our encapsulation approach. Beyond manufacturing and BMC, cost considerations include the choice of iron sulfate, because it is one of the lowest cost forms of iron (60) and because iron sulfate enables higher bioavailability as compared to other iron forms (61). Additional implications will require country-, region-, and/or individual-specific micronutrient needs, and careful attention must be paid to local public and regulatory policies to enable widespread use of this technology. The MP delivery system has been tested in vitro, in vivo in mice, and in humans and has been scaled up using commercially relevant processes. Furthermore, we have demonstrated the modularity and tunability of our platform by identifying and subsequently modifying the MPs to address absorption-limiting design criteria. In summary, a heat-stable pH-responsive polymer-based MP delivery system has been developed that shows promise as a platform for micronutrient delivery to humans.

MATERIALS AND METHODS
Study design
We hypothesized that a polymer-based MP encapsulation system that maintained micronutrient stability in boiling water for hours and rapidly releases micronutrient payloads in acidic stomach conditions could address challenges with micronutrient delivery. Hence, we studied micronutrient absorption in both rodents and human subjects to evaluate our MP technology. Animal studies were approved by the Institutional Animal Care and Use Committee and were performed at the Massachusetts Institute of Technology (MIT). For humans, two studies were performed using a single-blind, randomized, cross-over design. In study 1, three maize por-

ridge test meals were administered; in study 2, participants consumed nine wheat bread test meals. All test meals were labeled with 4 mg of Fe as $FeSO_4$ using stable iron isotopes (^{54}Fe, ^{57}Fe, or ^{58}Fe). Labeled $FeSO_4$ was prepared by Dr. Paul Lohmann GmbH (Germany) from isotopically ^{54}Fe-, ^{58}Fe-, and ^{57}Fe-enriched elemental iron (Chemgas, Boulogne, France). Particles used in study 1 were produced at MIT, and those used in study 2 were produced at Southwest Research Institute in San Antonio, Texas. Different participants were included in each study. After enrollment, each participant was allocated to a predefined schedule of test meal sequence and combinations in a randomized balanced block design. Each participant served as their own control. In study 1, the maize porridge test meals contained fortified salt, added either before or after cooking. The fortified salt contained either (i) $FeSO_4$ (reference), (ii) iron-loaded BMC-HA-Fe (0.6%) added before cooking, or (iii) iron-loaded BMC-HA-Fe (0.6%) added after cooking. In study 2, the wheat bread test meals were fortified before baking. The test meals contained either (i) iron-loaded BMC-HA-Fe (3.19%), (ii) iron-loaded BMC-HA-Fe (18.29%), (iii) iron-loaded HA-Fe (8.75%), (iv) iron-loaded BMC-HA-Fe (3.19%) with VitA-BMC (3.4%; 37.65 mg of vitamin A), (v) iron-loaded BMC-HA-Fe (3.19%) with VitA-BMC (3.4%; 37.65 mg of vitamin A) with free folic acid (0.34 mg), (vi) $FeSO_4$, (vii) $FeSO_4$ with HA [25.68 mg to match HA in group (i)], (viii) $FeSO4$ with BMC [85.19 mg to match BMC in group (i)], or (ix) $FeSO_4$ with BMC [85.19 mg to match BMC in group (i)] with HA [25.68 mg to match HA in group (i)]. Within 1 week, each participant consumed a test meal on three consecutive days, and after a 14-day (study 1) and 19-day (study 2) break, a blood sample was taken for measurement of stable iron isotope incorporation into the erythrocytes. In study 2, this procedure was repeated twice. The total study duration of study 1 was 17 days, and study 2 was 64 days. Participants were recruited among female students at the Swiss Federal Institute of Technology in Zürich and University of Zürich. Inclusion criteria were as follows: apparently healthy, nonpregnant (assessed by a pregnancy test), nonlactating, age between 18 and 40 years, weight <65 kg, body mass index of 18.5 to 25 kg/m^2, depleted iron status defined as a PF concentration of <20 mg/liter), and in the absence of systemic inflammation [defined with a C-reactive protein (CRP) concentration of >5 mg/liter]. Exclusion criteria were as follows: chronic disease or intake of long-term medication (except for oral contraceptives), consumption of mineral and vitamin supplements within the 2 weeks before first test meal administration, and significant blood loss or transfusion, within 4 months before the study initiation. Informed written consent was obtained from all participants. Ethical approval for both studies was provided by the ethical review committee of Cantonal Ethics Commission of Zürich (study 1, KEK-ZH-Nr. 2015-0094; study 2, KEK-ZH-Nr. 2017-01624) and the Committee on the Use of Humans as Experimental Subjects at MIT (study 1, COUHES #1502006932; study 2, COUHES #1801201448/1801201448A001); both trials were registered on ClinicalTrials.gov: study 1 (NCT02353325) and study 2 (NCT03332602). Both studies were powered to detect a nutritionally relevant, 30% within-group difference in iron absorption, based on an SD of 0.35 from log-transformed iron absorption from previous studies by our laboratory (62), an α level of 5% (two-tailed), and 80% power; 18 subjects were calculated. In study 1, a 10% dropout rate was anticipated; in study 2, because of the longer duration of the study, a 30% dropout rate was anticipated; therefore, 20 and 24 subjects were recruited, respectively.

Anselmo et al., Sci. Transl. Med. 11, eaaw3680 (2019)   13 November 2019

9 of 13

Formulation of one-step MPs (BMC MPs) and two-step MPs (HA-BMC MPs)

BMC MPs were prepared by a modified oil/water emulsion method (63). The organic phase for the emulsion consisted of either (i) 1 mg of blank or dye-labeled HA MPs homogeneously dispersed in 1 ml of BMC solution (100 mg/ml) in methylene chloride; (ii) vitamin A (10 mg/ml), vitamin D (2 mg/ml), folic acid–loaded HA MPs (1.3 mg), and B12-loaded HA MPs (1.3 mg) dissolved into BMC solution (100 mg/ml, 1 ml) in methylene chloride to prepare BMC MPs co-encapsulated with four different types of micronutrients; (iii) HA MPs encapsulated with various micronutrients as described in table S2 to synthesize HA-BMC MPs with various micronutrient loads; (iv) free micronutrients as described in table S2 to synthesize BMC MPs with various micronutrient loads; or (v) lipophilic carbocyanine DiOC18(7) dye (1 mg/ml) (DiR, Life Technologies) and BMC (100 mg/ml) in methylene chloride to synthesize fluorescently labeled BMC MPs. The resulting organic phases were then emulsified in polyvinyl alcohol (PVA) solution (20 ml, 10 mg/ml) with a stirring rate at 300 rpm for 10 min. The obtained emulsion was added into 100 ml of deionized water with stirring (500 rpm for 10 min) to solidify the MPs. The obtained MPs were allowed to settle by gravity and thoroughly washed with water. The final dry MPs were obtained by lyophilization.

Micronutrient-MP loading, release, and stability

Vitamins B2, niacin, folic acid, B12, A, and D were analyzed via high-performance liquid chromatography (Agilent 1100; Agilent Technologies) using a C-18 column (Acclaim Polar Advantage II, 3 µm, 4.6 mm × 150 mm) and were detected by a photodiode detector at 265, 265, 286, 550, 325, and 264 nm, respectively. Iron, biotin, zinc, and vitamin C were analyzed using BioVision colorimetric assay kits, and vitamin biotin was analyzed using a Sigma colorimetric assay kit. Iodine was measured using UV-visible absorbance at 288 nm. DiR-loaded BMC MPs were dissolved in dimethyl sulfoxide, and then the dissolved cargo was quantified using a multimode reader (TECAN Infinite M200 PRO) at 750 nm. Micronutrient-loaded HA MPs were dissolved in water, and micronutrient content was determined as described above for each respective micronutrient. To quantify micronutrient loading in the co-encapsulated HA-BMC MPs or the BMC MPs, a known mass of MPs was first dissolved in SGF and then analyzed for the total micronutrient mass. The precipitated BMC was removed via centrifugation using Amicon Ultra centrifugal filters (3000 normal molecular weight limit) at 14,000g for 30 min to remove HA and BMC. The dissolved micronutrients were separated and quantified as described above. To quantify vitamin A and D loading, the MPs were dissolved in methylene chloride and the dissolved vitamins A and D were separated and quantified as described above. The release profiles of micronutrients were studied in water at RT, boiling water at 100°C, and SGF at 37°C. At each time point, samples were centrifuged at 4000 rpm for 5 min, and 900 µl of the supernatant was collected for analysis, and then samples were replenished with 900 µl of fresh release medium. For vitamins A and D, the aqueous release medium was brought into contact with a layer of methylene chloride, and then the extracted fat-soluble vitamins within the organic phase were used for analysis. The cumulative release was calculated as the total amount of micronutrient released at a particular time point relative to the amount initially loaded. Dry micronutrients were dispersed in water and then heated at 100°C for 2 hours before being centrifuged at 4000 rpm for 5 min. The stability percent-age equals the ratio of stable micronutrient after to the actual loading of the micronutrient in the MPs. For samples in unencapsulated form, they were either dissolved in water or dispersed in water before being heated for 2 hours. The sensory performance was measured in duplicate as the absolute color change in a food matrix after the addition of the Fe microspheres. A banana milk slurry was chosen as polyphenol-rich food matrix. The fortificants were added to 70 g of banana milk at a concentration of 60 ppm Fe in banana milk. The banana milk was prepared fresh: 180 g of fresh banana with 520 g of organic whole milk (3.9% fat, homogenized, pasteurized). Color change was measured in duplicate at baseline (before fortification) and 2 hours after fortification and stirring at 350 rpm. The absolute color change of ΔE was measured and calculated as previously described (64). FeSO4 and ferric pyrophosphate (FePP; 20% Fe, micronized powder) were used as positive and negative controls.

Dissolution study of DiR-loaded BMC MPs in mice

Female SKH1-Elite mice (Crl:SKH1-hr) were purchased from Charles River Laboratories at 8 to 12 weeks of age. Mice were fed an alfalfa-free balanced diet (Harlan Laboratories, AIN-76A) for 10 days before treatment to reduce food-related autofluorescence. About 200 mg of DiR-loaded BMC MPs was administered in 100 µl of water via gavage (n = 3). After 15, 30, or 60 min, mice were euthanized using carbon dioxide asphyxiation. The gastrointestinal tract was immediately explanted and imaged using in vivo imaging system (IVIS, PerkinElmer). The fluorescent signals from mice that had ingested DiR-loaded BMC MPs were compared to mice that did not receive MPs. The spectral signatures associated with encapsulated and released DiR were then computationally separated from tissue autofluorescence (identified in the control samples) to determine the location and status of dye release. Quantified signal/background ratios were determined by normalizing the encapsulated or released dye signal, in either the stomach or intestines, to a background in control animals receiving no BMC MPs.

In vivo vitamin A absorption in rats

Tritium-labeled retinyl palmitate (American Radiolabeled Chemicals Inc.) was used to detect the amount of absorbed vitamin A in blood. Radiolabeled VitA-BMC MPs were prepared by the oil/water emulsion method described above. Female Wistar rats (~250 g) were purchased from Charles River Laboratories. The rats were divided into two groups: (i) free vitamin A and (ii) VitA-BMC MPs. In the free group, vitamin A was delivered in a 4% (v/v) ethanol/water mixture to enable solubilization of vitamin A. The VitA-BMC MPs were dispersed in water and vortexed to form a suspension. Each rat was oral gavaged 10 µCi of vitamin A in either its free form or encapsulated MPs in 350 µl of either ethanol/water mixture or water total. Residual vitamin A in the syringe and gavage needle was saved and quantified by scintillation counter to calculate the actual feeding amount of tritium-labeled retinyl palmitate for each rat. At 0.5, 1, 2, 3, 4, 5, and 6 hours, the rats were anesthetized via isoflurane and 200 µl of blood was collected from the lateral tail vein. The radioactivity in the samples was quantified via liquid scintillation counting with a Tri-Carb 2810 TR liquid scintillation counter. To calculate loading of vitamin A in the VitA-BMC MPs, the MPs were first dissolved in 1 ml of DCM, and then 5 µl of the solution was mixed with 10 ml of an Ultima Gold F liquid scintillation cocktail (PerkinElmer Inc.). Blood (200 µl) was dissolved in SOLVABLE (PerkinElmer Inc.) following recommended protocol, and then

1 ml of the dissolved blood was mixed with 10 ml of Hionic-Fluor liquid scintillation cocktail.

MatTek EpiIntestinal transport

EpiIntestinal tissues were purchased from MatTek (Ashland) and used as recommended. For transport experiments, the particle constituents BMC, Fe, and HA were separately prepared and added to achieve final mass percentages as reported. After 1 hour of incubation at 37°C and 5% CO_2, transport iron was analyzed in the bottom transwell chamber using the previously described BioVision colorimetric assay.

Process development and scale-up

The detailed process described here was used to manufacture 1 kg of Fe-HA-BMC MPs as shown in Fig. 6. A Niro Production Minor pilot scale spray dryer was used to first prepare Fe-HA MPs. The feed solution contained 525.5 g of sodium hyaluronate, 1309.5 g of iron sulfate monohydrate, and 77 liters of deionized water. This solution was fed into the dryer at 250 g/min and atomized with a 2-mm two-fluid nozzle. The dryer inlet temperature was set to 257°C, resulting in an outlet temperature of 90°C. MPs (1215 g) were recovered. Fe-HA MPs were encapsulated with BMC using a custom spinning disc atomization system. The feed solution was prepared with 1152 g of BMC and 1.87 g of polysorbate 80 dissolved in 12,000 g of DCM. Fe-HA MPs (48 g) were added to the DCM solution and placed in a sonication bath for 10 min to form a stable suspension. The suspension was fed at 110 g/min onto a 10.16-cm-diameter stainless steel custom disc spinning at 1300 rpm. The disc was mounted 9.144 m high in a 6.096 m × 6.096 m tower. The room was heated to 35° to 40°C. Particles were collected on antistatic plastic located at the bottom of the tower. MPs (1059 g) were recovered. These processes were modified for batches used in human study 2 by using a ProCepT 4 M8 laboratory spray dryer for the Fe-HA MPs. All new tubing and filters were used with the spray dryer, in addition to cleaning all wetted parts with soapy water and a 70% aqueous isopropanol solution. The inlet temperature for the spray dryer was set to 160°C, resulting in an outlet temperature of about 53°C. Solution was dried at 8 ml/min through a 0.4-mm air-atomized nozzle. The same spinning disc setup was used for encapsulating the Fe-HA MPs within BMC. The tower was mopped and cleaned, followed by treatment with Vesphene IIse. Encapsulated vitamin A for feed studies was also prepared using the same spinning disc system. A disc speed of 1675 rpm was used, as the feed solution was fed to a 10.16 cm spinning disc at about 115 g/min. The material was collected in a powdered Dry-Flo starch. The excess starch was then sieved from the sample to recover the vitamin A MPs. All samples were placed under vacuum with a slow N_2 purge for 1 week to remove residual DCM. Specific feed conditions for the MPs used in human study 2 are listed in table S4.

Statistical analysis

For in vitro and rodent studies, all quantitative measurements were performed on three independent replicates. All values are expressed as means ± SD. Statistical significance was evaluated using a two-tailed Student's t test. Statistical analysis of the human studies was done using SPSS version 22 (human study 1) and version 24 (human study 2) (IBM SPSS Statistics). All data were checked for normal distribution before analysis: Age, weight, height, Hb, and CRP were normal, and the data are presented as means and SD. PF and fractional Fe absorption are non-normal and are presented as geometric means and 95% CI. Comparisons between meals were done using the square root–transformed data fitted in a linear mixed model. Meals were entered as a repeated fixed factor (covariance type of scaled identity) and subjects as random factors (intercept). If a significant overall effect of meals was found, post hoc tests within different meals were performed using the Bonferroni correction for multiple comparisons. $P < 0.05$ was considered statistically different.

REFERENCES AND NOTES

1. K. M. Jamil, A. S. Rahman, P. Bardhan, A. I. Khan, F. Chowdhury, S. A. Sarker, A. M. Khan, T. Ahmed, Micronutrients and anaemia. *J. Health Popul. Nutr.* **26**, 340–355 (2008).

2. S. S. Lim, T. Vos, A. D. Flaxman, G. Danaei, K. Shibuya, H. Adair-Rohani, M. Amann, H. R. Anderson, K. G. Andrews, M. Aryee, C. Atkinson, L. J. Bacchus, A. N. Bahalim, K. Balakrishnan, J. Balmes, S. Barker-Collo, A. Baxter, M. L. Bell, J. D. Blore, F. Blyth, C. Bonner, G. Borges, R. Bourne, M. Boussinesq, M. Brauer, P. Brooks, N. G. Bruce, B. Brunekreef, C. Bryan-Hancock, C. Bucello, R. Buchbinder, F. Bull, R. T. Burnett, T. E. Byers, B. Calabria, J. Carapetis, E. Carnahan, Z. Chafe, F. Charlson, H. Chen, J. S. Chen, A. T. Cheng, J. C. Child, A. Cohen, K. E. Colson, B. C. Cowie, S. Darby, S. Darling, A. Davis, L. Degenhardt, F. Dentener, D. C. D. Jarlais, K. Devries, M. Dherani, E. L. Ding, E. R. Dorsey, T. Driscoll, K. Edmond, S. E. Ali, R. E. Engell, P. J. Erwin, S. Fahimi, G. Falder, F. Farzadfar, A. Ferrari, M. M. Finucane, S. Flaxman, F. G. Fowkes, G. Freedman, M. K. Freeman, E. Gakidou, S. Ghosh, E. Giovannucci, G. Gmel, K. Graham, R. Grainger, B. Grant, D. Gunnell, H. R. Gutierrez, W. Hall, H. W. Hoek, A. Hogan, H. D. Hosgood 3rd, D. Hoy, H. Hu, B. J. Hubbell, S. J. Hutchings, S. E. Ibeanusi, G. L. Jacklyn, R. Jasrasaria, J. B. Jonas, H. Kan, J. A. Kanis, N. Kassebaum, N. Kawakami, Y. H. Khang, S. Khatibzadeh, J. P. Khoo, C. Kok, F. Laden, R. Lalloo, Q. Lan, T. Lathlean, J. L. Leasher, J. Leigh, Y. Li, J. K. Lin, S. E. Lipshultz, S. London, R. Lozano, Y. Lu, J. Mak, R. Malekzadeh, L. Mallinger, W. Marcenes, L. March, R. Marks, R. Martin, P. McGale, J. McGrath, S. Mehta, G. A. Mensah, T. R. Merriman, R. Micha, C. Michaud, V. Mishra, K. M. Hanafiah, A. A. Mokdad, L. Morawska, D. Mozaffarian, T. Murphy, M. Naghavi, B. Neal, P. K. Nelson, J. M. Nolla, R. Norman, C. Olives, S. B. Omer, J. Orchard, R. Osborne, B. Ostro, A. Page, K. D. Pandey, C. D. Parry, E. Passmore, J. Patra, N. Pearce, P. M. Pelizzari, M. Petzold, M. R. Phillips, D. Pope, C. A. Pope 3rd, J. Powles, M. Rao, H. Razavi, E. A. Rehfuess, J. T. Rehm, B. Ritz, F. P. Rivara, T. Roberts, C. Robinson, J. A. Rodriguez-Portales, I. Romieu, R. Room, L. C. Rosenfeld, A. Roy, L. Rushton, J. A. Salomon, U. Sampson, L. Sanchez-Riera, E. Sanman, A. Sapkota, S. Seedat, P. Shi, K. Shield, R. Shivakoti, G. M. Singh, D. A. Sleet, E. Smith, K. R. Smith, N. J. Stapelberg, K. Steenland, H. Stockl, L. J. Stovner, K. Straif, L. Straney, G. D. Thurston, J. H. Tran, R. Van Dingenen, A. van Donkelaar, J. L. Veerman, L. Vijayakumar, R. Weintraub, M. M. Weissman, R. A. White, H. Whiteford, S. T. Wiersma, J. D. Wilkinson, H. C. Williams, W. Williams, N. Wilson, A. D. Woolf, P. Yip, J. M. Zielinski, A. D. Lopez, C. J. Murray, M. Ezzati, M. A. AlMazroa, Z. A. Memish, A comparative risk assessment of burden of disease and injury attributable to 67 risk factors and risk factor clusters in 21 regions, 1990-2010: A systematic analysis for the Global Burden of Disease Study 2010. *Lancet* **380**, 2224–2260 (2012).

3. M. B. Zimmermann, P. L. Jooste, C. S. Pandav, Iodine-deficiency disorders. *Lancet* **372**, 1251–1262 (2008).

Anselmo *et al.*, *Sci. Transl. Med.* **11**, eaaw3680 (2019)   13 November 2019

11 of 13

4. F. A. Oski, Iron deficiency in infancy and childhood. *N. Engl. J. Med.* **329**, 190–193 (1993).

5. E. M. Wiseman, S. Bar-El Dadon, R. Reifen, The vicious cycle of vitamin A deficiency: A review. *Crit. Rev. Food Sci. Nutr.* **57**, 3703–3714 (2017).

6. D. O. Kennedy, B vitamins and the brain: Mechanisms, dose and efficacy—A review. *Nutrients* **8**, 68 (2016).

7. N. E. Palermo, M. F. Holick, Vitamin D, bone health, and other health benefits in pediatric patients. *J. Pediatr. Rehabil. Med.* **7**, 179–192 (2014).

8. R. Black, Micronutrient deficiency: An underlying cause of morbidity and mortality. *Bull. World Health Organ.* **81**, 79 (2003).

9. F. J. Levinson, L. Bassett, *Malnutrition Is Still a Major Contributor to Child Deaths* (Population Reference Bureau, 2007).

10. Z. A. Bhutta, R. A. Salam, Global nutrition epidemiology and trends. *Ann. Nutr. Metab.* **61**, 19–27 (2013).

11. A. M. Leung, L. E. Braverman, E. N. Pearce, History of U.S. iodine fortification and supplementation. *Nutrients* **4**, 1740–1746 (2012).

12. K. Charlton, S. Skeaff, Iodine fortification: Why, when, what, how, and who? *Curr. Opin. Clin. Nutr.* **14**, 618–624 (2011).

13. G. Arroyave, L. A. Mejia, J. R. Aguilar, The effect of vitamin A fortification of sugar on the serum vitamin A levels of preschool Guatemalan children: A longitudinal evaluation. *Am. J. Clin. Nutr.* **34**, 41–49 (1981).

14. C. Liyanage, S. Zlotkin, Bioavailability of iron from micro-encapsulated iron sprinkle supplement. *Food Nutr. Bull.* **23**, 133–137 (2002).

15. M. B. Zimmermann, The potential of encapsulated iron compounds in food fortification: A review. *Int. J. Vitam. Nutr. Res.* **74**, 453–461 (2004).

16. I. Raileanu, L. L. Diosady, Vitamin A stability in salt triple fortified with iodine, iron, and vitamin A. *Food Nutr. Bull.* **27**, 252–259 (2006).

17. P. Sauvant, M. Cansell, A. Hadj Sassi, C. Atgié, Vitamin A enrichment: Caution with encapsulation strategies used for food applications. *Food Res. Int.* **46**, 469–479 (2012).

18. D. Moretti, M. Zimmermann, Assessing bioavailability and nutritional value of microencapsulated minerals, in *Encapsulation and Controlled Release Technologies in Food Systems*, J. M. Lakkis, Ed. (John Wiley & Sons, 2016).

19. R. L. Bailey, K. P. West Jr., R. E. Black, The epidemiology of global micronutrient deficiencies. *Ann. Nutr. Metab.* **66**, 22–33 (2015).

20. M. Andersson, V. Karumbunathan, M. B. Zimmermann, Global iodine status in 2011 and trends over the past decade. *J. Nutr.* **142**, 744–750 (2012).

21. R. E. Black, in *International Nutrition: Achieving Millennium Goals and Beyond* (Karger Publishers, 2014), vol. 78, pp. 21–28.

22. L. H. Allen, *Hidden Hunger* (Karger Publishers, 2016), vol. 115, pp. 109–117.

23. F. E. Runge, R. Heger, Use of microcalorimetry in monitoring stability studies. Example: Vitamin A esters. *J. Agric. Food Chem.* **48**, 47–55 (2000).

24. I. Van den Broeck, L. Ludikhuyze, C. Weemaes, A. Van Loey, M. Hendrickx, Kinetics for isobaric-isothermal degradation ʟ-ascorbic acid. *J. Agric. Food Chem.* **46**, 2001–2006 (1998).

25. M. Allwood, J. Plane, The wavelength-dependent degradation of vitamin A exposed to ultraviolet radiation. *Int. J. Pharm.* **31**, 1–7 (1986).

26. C. V. Moore, R. Dubach, V. Minnich, H. K. Roberts, Absorption of ferrous and ferric radioactive iron by human subjects and by dogs. *J. Clin. Investig.* **23**, 755–767 (1944).

27. H. Kwak, K. Yang, J. Ahn, Microencapsulated iron for milk fortification. *J. Agric. Food Chem.* **51**, 7770–7774 (2003).

28. D. J. McClements, E. A. Decker, J. Weiss, Emulsion-based delivery systems for lipophilic bioactive components. *J. Food Sci.* **72**, R109–R124 (2007).

29. Y. O. Li, L. L. Diosady, A. S. Wesley, Folic acid fortification through existing fortified foods: Iodized salt and vitamin A-fortified sugar. *Food Nutr. Bull.* **32**, 35–41 (2011).

30. D. J. McClements, Nanoscale nutrient delivery systems for food applications: Improving bioactive dispersibility, stability, and bioavailability. *J. Food Sci.* **80**, N1602–N1611 (2015).

31. R. Y. Yada, N. Buck, R. Canady, C. DeMerlis, T. Duncan, G. Janer, L. Juneja, M. Lin, D. J. McClements, G. Noonan, J. Oxely, C. Sablivo, L. Tsytsikova, S. Vázquez-Campos, J. Yourick, Q. Zhong, S. Thurmond, Engineered nanoscale food ingredients: Evaluation of current knowledge on material characteristics relevant to uptake from the gastrointestinal tract. *Compr. Rev. Food Sci. Food Saf.* **13**, 730–744 (2014).

32. J. Yi, Y. Fan, W. Yokoyama, Y. Zhang, L. Zhao, Thermal degradation and isomerization of β-carotene in oil-in-water nanoemulsions supplemented with natural antioxidants. *J. Agric. Food Chem.* **64**, 1970–1976 (2016).

33. Y. O. Li, D. Yadava, K. L. Lo, L. L. Diosady, A. S. Wesley, Feasibility and optimization study of using cold-forming extrusion process for agglomerating and microencapsulating ferrous fumarate for salt double fortification with iodine and iron. *J. Microencapsul.* **28**, 639–649 (2011).

34. M. Bogataj, A. Mrhar, A. Kristl, F. Kozjek, Preparation and evaluation of Eudragit E microspheres containing bacampicillin. *Drug Dev. Ind. Pharm.* **15**, 2295–2313 (1989).

35. M. Lorenzo-Lamosam, M. Cuña, L. Vila-Jatod, D. Torres, M. Alonso, Development of a microencapsulated form of cefuroxime axetil using pH-sensitive acrylic polymers. *J. Microencapsul.* **14**, 607–616 (1997).

36. R. Schellekens, F. Stellaard, D. Mitrovic, F. Stuurman, J. Kosterink, H. Frijlink, Pulsatile drug delivery to ileo-colonic segments by structured incorporation of disintegrants in pH-responsive polymer coatings. *J. Control. Release* **132**, 91–98 (2008).

37. R. Mustafin, Interpolymer combinations of chemically complementary grades of Eudragit copolymers: A new direction in the design of peroral solid dosage forms of drug delivery systems with controlled release (review). *Pharm. Chem. J.* **45**, 285–295 (2011).

38. R. Moustafine, A. V. Bukhovets, A. Sitenkov, V. Kemenova, P. Rombaut, G. van den Mooter, Eudragit E PO as a complementary material for designing oral drug delivery systems with controlled release properties: Comparative evaluation of new interpolyelectrolyte complexes with countercharged eudragit L100 copolymers. *Mol. Pharm.* **10**, 2630–2641 (2013).

39. B. Karolewicz, A review of polymers as multifunctional excipients in drug dosage form technology. *Saudi Pharm. J.* **24**, 525–536 (2015).

40. J. Eisele, G. Haynes, K. Kreuzer, C. Hall, Toxicological assessment of anionic methacrylate copolymer: I. characterization, bioavailability and genotoxicity. *Regul. Toxicol. Pharmacol.* **82**, 39–47 (2016).

41. P. Li, Z. Yang, Y. Wang, Z. Peng, S. Li, L. Kong, Q. Wang, Microencapsulation of coupled folate and chitosan nanoparticles for targeted delivery of combination drugs to colon. *J. Microencapsul.* **32**, 40–45 (2014).

42. M. Haham, S. Ish-Shalom, M. Nodelman, I. Duek, E. Segal, M. Kustanovich, Y. D. Livney, Stability and bioavailability of vitamin D nanoencapsulated in casein micelles. *Food Funct.* **3**, 737–744 (2012).

43. R. I. Mellican, J. Li, H. Mehansho, S. S. Nielsen, The role of iron and the factors affecting off-color development of polyphenols. *J. Agric. Food Chem.* **51**, 2304–2316 (2003).

44. C. Z. Ran, A. Moore, Spectral unmixing imaging of wavelength-responsive fluorescent probes: An application for the real-time report of amyloid β species in Alzheimer's disease. *Mol. Imaging Biol.* **14**, 293–300 (2012).

45. L. Hallberg, M. Brune, L. Rossander, Iron absorption in man: Ascorbic acid and dose-dependent inhibition by phytate. *Am. J. Clin. Nutr.* **49**, 140–144 (1989).

46. I. Maschmeyer, T. Hasenberg, A. Jaenicke, M. Lindner, A. K. Lorenz, J. Zech, L. A. Garbe, F. Sonntag, P. Hayden, S. Ayehunie, R. Lauster, U. Marx, E. M. Materne, Chip-based human liver-intestine and liver-skin co-cultures—A first step toward systemic repeated dose substance testing in vitro. *Eur. J. Pharm. Biopharm.* **95**, 77–87 (2015).

47. J. P. Wikswo, The relevance and potential roles of microphysiological systems in biology and medicine. *Exp. Biol. Med.* **239**, 1061–1072 (2014).

48. C. P. Reis, R. J. Neufeld, A. J. Ribeiro, F. Veiga, Nanoencapsulation I. Methods for preparation of drug-loaded polymeric nanoparticles. *Nanomedicine* **2**, 8–21 (2006).

49. J. B. Dressman, R. R. Berardi, L. C. Dermentzoglou, T. L. Russell, S. P. Schmaltz, J. L. Barnett, K. M. Jarvenpaa, Upper gastrointestinal (GI) pH in young, healthy men and women. *Pharm. Res.* **7**, 756–761 (1990).

50. S. Thakral, N. K. Thakral, D. K. Majumdar, Eudragit: A technology evaluation. *Expert Opin. Drug Deliv.* **10**, 131–149 (2013).

51. D. Klimkowsky, *Moisture Protection and Taste-Masking with Polymethacrylate Coatings* (Evonik Industries, 2008); http://www.phexcom.cn/uploadfiles/200899112713336.pdf.

52. A. A. Kader, D. Zagory, E. L. Kerbel, C. Y. Wang, Modified atmosphere packaging of fruits and vegetables. *Crit. Rev. Food Sci. Nutr.* **28**, 1–30 (1989).

53. E.-C. Cho, Effect of polymer characteristics on the thermal stability of retinol encapsulated in aliphatic polyester nanoparticles. *Bull. Kor. Chem. Soc.* **33**, 2560–2566 (2012).

54. J. Eisele, G. Haynes, T. Rosamilia, Characterisation and toxicological behaviour of basic methacrylate copolymer for GRAS evaluation. *Regul. Toxicol. Pharmacol.* **61**, 32–43 (2011).

55. K. Ramalakshmi, B. Raghavan, Caffeine in coffee: Its removal. Why and how? *Crit. Rev. Food Sci. Nutr.* **39**, 441–456 (1999).

56. Joint FAO/WHO Expert Committee on Food Additives, Summary and Conclusions, 86th Meeting, Geneva, 12 to 21 June 2018.

57. Report of the 51st Session of the Codex Committee on Food Additives, Jinan, China, 25 to 29 March 2019.

58. B. Sandström, Micronutrient interactions: Effects on absorption and bioavailability. *Br. J. Nutr.* **85**, S181–S185 (2001).

59. R. Murugesan, V. Orsat, Spray drying for the production of nutraceutical ingredients— A review. *Food Bioprocess Technol.* **5**, 3–14 (2012).

60. O. Schröder, O. Mickisch, U. Seidler, A. De Weerth, A. U. Dignass, H. Herfarth, M. Reinshagen, S. Schreiber, U. Junge, M. Schrott, J. Stein, Intravenous iron sucrose versus oral iron supplementation for the treatment of iron deficiency anemia in patients with inflammatory bowel disease—A randomized, controlled, open-label, multicenter study. *Am. J. Gastroenterol.* **100**, 2503–2509 (2005).

61. A. B. Pérez-Expósito, S. Villalpando, J. A. Rivera, I. J. Griffin, S. A. Abrams, Ferrous sulfate is more bioavailable among preschoolers than other forms of iron in a milk-based weaning food distributed by PROGRESA, a national program in Mexico. *J. Nutr.* **135**, 64–69 (2005).

62. I. Herter-Aeberli, K. Eliancy, Y. Rathon, C. U. Loechl, J. M. Pierre, M. B. Zimmermann, In Haitian women and preschool children, iron absorption from wheat flour–based meals fortified with sodium iron EDTA is higher than that from meals fortified with ferrous fumarate, and is not affected by Helicobacter pylori infection in children. *Br. J. Nutr.* **118**, 273–279 (2017).

63. T. Kemala, E. Budianto, B. Soegiyono, Preparation and characterization of microspheres based on blend of poly(lactic acid) and poly(ε-caprolactone) with poly(vinyl alcohol) as emulsifier. *Arab. J. Chem.* **5**, 103–108 (2012).

64. Y. Shen, L. Posavec, S. Bolisetty, F. M. Hilty, G. Nystrom, J. Kohlbrecher, M. Hilbe, A. Rossi, J. Baumgartner, M. B. Zimmermann, R. Mezzenga, Amyloid fibril systems reduce, stabilize and deliver bioavailable nanosized iron. *Nat. Nanotechnol.* **12**, 642–647 (2017).

65. A. K. Jha, X. A. Xu, R. L. Duncan, X. Q. Jia, Controlling the adhesion and differentiation of mesenchymal stem cells using hyaluronic acid-based, doubly crosslinked networks. *Biomaterials* **32**, 2466–2478 (2011).

66. X. Q. Jia, Y. Yeo, R. J. Clifton, T. Jiao, D. S. Kohane, J. B. Kobler, S. M. Zeitels, R. Langer, Hyaluronic acid-based microgels and microgel networks for vocal fold regeneration. *Biomacromolecules* **7**, 3336–3344 (2006).

67. A. K. Jha, R. A. Hule, T. Jiao, S. S. Teller, R. J. Clifton, R. L. Duncan, D. J. Pochan, X. Q. Jia, Structural analysis and mechanical characterization of hyaluronic acid-based doubly cross-linked networks. *Macromolecules* **42**, 537–546 (2009).

68. R. U. Makower, Extraction and determination of phytic acid in beans (Phaseolus-Vulgaris). *Cereal Chem.* **47**, 288 (1970).

69. World Health Organization, *Iron Deficiency Anaemia: Assessment, Prevention and Control: A Guide for Programme Managers* (World Health Organization, 2001), 114 pp.

70. C. I. Cercamondi, I. M. Egli, E. Mitchikpe, F. Tossou, C. Zeder, J. D. Hounhouigan, R. F. Hurrell, Total iron absorption by young women from iron-biofortified pearl millet composite meals is double that from regular millet meals but less than that from post-harvest iron-fortified millet meals. *J. Nutr.* **143**, 1376–1382 (2013).

71. E. Brown, B. Bradley, R. Wennesland, J. L. Hodges Jr., J. Hopper, H. Yamauchi, Red cell, plasma, and blood volume in healthy women measured by radiochromium cell-labeling and hematocrit. *J. Clin. Invest.* **41**, 2182–2190 (1962).

72. V. Kumar, T. Yang, Y. Yang, Interpolymer complexation. I. Preparation and characterization of a polyvinyl acetate phthalate-polyvinylpyrrolidone (PVAP-PVP) complex. *Int. J. Pharm.* **188**, 221–232 (1999).

73. Colorcon, OPADRY® Enteric: Acrylic-Based Coating System – 91 Series (2019); https://www.colorcon.com/products-formulation/all-products/download/747/2093/34?method=view.

74. Eastman, Eastman C-A-P enteric coating materials (Cellulose acetate phthalate or cellacefate, NF) (2016); http://www.eastman.com/Literature_Center/C/CECOAT3143.pdf.

75. P. Roxin, A. Karlsson, S. K. Singh, Characterization of cellulose acetate phthalate (CAP). *Drug Dev. Ind. Pharm.* **24**, 1025–1041 (1998).

76. C. Malm, J. Emerson, G. D. Hiatt, Cellulose acetate phthalate as an enteric coating material. *J. Am. Pharm. Assoc.* **40**, 520–525 (1951).

77. ShinEtsu, USP Hypromellose Phthalate HPMCP (2002); http://www.metolose.ru/files/hpmcp.pdf.

78. K. Thoma, K. Bechtold, Influence of aqueous coatings on the stability of enteric coated pellets and tablets. *Eur. J. Pharm. Biopharm.* **47**, 39–50 (1999).

79. ShinEtsu, Hypromellose Acetate Succinate: Shin-Etsu AQOAT (2005); http://www.elementoorganika.ru/files/aqoat.

80. Z. Dong, D. S. Choi, Hydroxypropyl methylcellulose acetate succinate: Potential drug–excipient incompatibility. *AAPS PharmSciTech* **9**, 991–997 (2008).

81. Swadeshi International Company, Dewaxed Decolourised Shellac (Flakes); http://www.shellac.in/shellac_machinemade.html.

82. Y. Farag, C. Leopold, Physicochemical properties of various shellac types. *Dissolut. Technol.* **16**, 33–39 (2009).

83. S. Limmatvapirat, C. Limmatvapirat, S. Puttipipatkhachorn, J. Nuntanid, M. Luangtana-anan, Enhanced enteric properties and stability of shellac films through composite salts formation. *Eur. J. Pharm. Biopharm.* **67**, 690–698 (2007).

84. A. Patel, P. Heussen, J. Hazekamp, K. P. Velikov, Stabilisation and controlled release of silibinin from pH responsive shellac colloidal particles. *Soft Matter* **7**, 8549–8555 (2011).

85. M. L. Aldridge, Re: Docket No. 02N-0434 Withdrawal of Certain Proposed Rules and Other Proposed Actions; Notice of Intent (2003); https://www.fda.gov/ohrms/dockets/dailys/03/jul03/072803/02n-0434-c000017-vol3.pdf.

86. Kitozyme, Chitosan GRAS Notice (2011); https://www.fda.gov/downloads/Food/IngredientsPackagingLabeling/GRAS/NoticeInventory/ucm277279.pdf.

87. C. Qin, H. Li, Q. Xiao, Y. Liu, J. Zhu, Y. Du, Water-solubility of chitosan and its antimicrobial activity. *Carbohydr. Polym.* **63**, 367–374 (2006).

88. E. Szymańska, K. Winnicka, Stability of chitosan—A challenge for pharmaceutical and biomedical applications. *Mar. Drugs* **13**, 1819–1846 (2015).

89. Evonik, Eudragit® Polymers – Defining Targeted Drug Release; http://healthcare.evonik.com/sites/lists/NC/DocumentsHC/Evonik-Eudragit_brochure.pdf.

90. C. N. Patra, R. Priya, S. Swain, G. K. Jena, K. C. Panigrahi, D. Ghose, Pharmaceutical significance of Eudragit: A review. *Fut. J. Pharma. Sci.* **3**, 33–45 (2017).

91. Evonik, Advanced Functional Coating Solutions for Nutraceuticals; http://healthcare.evonik.com/sites/lists/NC/DocumentsHC/Evonik_EUDRAGUARD%20nutritional%20coating%20solutions_brochure.pdf.

92. Evonik, EUDRAGIT® E 100, EUDRAGIT® E PO and EUDRAGIT® E 12,5 (2015); https://www.pharma-excipients.ch/app/download/10453336098/TI-EUDRAGIT-E-100-E-PO-E-12-5-EN.pdf?t=1459521322.

Science Translational Medicine

A heat-stable microparticle platform for oral micronutrient delivery

Aaron C. Anselmo, Xian Xu, Simone Buerkli, Yingying Zeng, Wen Tang, Kevin J. McHugh, Adam M. Behrens, Evan Rosenberg, Aranda R. Duan, James L. Sugarman, Jia Zhuang, Joe Collins, Xueguang Lu, Tyler Graf, Stephany Y. Tzeng, Sviatlana Rose, Sarah Acolatse, Thanh D. Nguyen, Xiao Le, Ana Sofia Guerra, Lisa E. Freed, Shelley B. Weinstock, Christopher B. Sears, Boris Nikolic, Lowell Wood, Philip A. Welkhoff, James D. Oxley, Diego Moretti, Michael B. Zimmermann, Robert Langer and Ana Jaklenec

Mitigating micronutrient deficiency

Particularly within the developing world, micronutrient deficiencies that impair growth and contribute to disease remain leading public health concerns. Although fortification of food can help treat deficiencies, heat used during cooking and other conditions can degrade vitamins, preventing adequate absorption. Anselmo and colleagues used the polymer BMC to encapsulate micronutrients. Microparticles encapsulating 11 micronutrients showed improved stability against oxidation, heat (such as boiling water used for cooking), and other conditions, and micronutrients were absorbed by the intestine when microparticles were administered to rodents. Data from two clinical trials and experiments using human intestinal tissue demonstrate how microparticle formulations were optimized to enhance iron loading, improve bioavailability, retain stability against cooking, and allow for scale-up. This microparticle platform could help improve oral delivery of micronutrients.

ARTICLE TOOLS	http://stm.sciencemag.org/content/11/518/eaaw3680
SUPPLEMENTARY MATERIALS	http://stm.sciencemag.org/content/suppl/2019/11/11/11.518.eaaw3680.DC1
RELATED CONTENT	http://stm.sciencemag.org/content/scitransmed/8/365/365ra157.full http://stm.sciencemag.org/content/scitransmed/11/488/eaau8581.full http://stm.sciencemag.org/content/scitransmed/11/483/eaau6753.full http://stm.sciencemag.org/content/scitransmed/9/390/eaal4069.full http://stm.sciencemag.org/content/scitransmed/7/275/275ra23.full
REFERENCES	This article cites 74 articles, 5 of which you can access for free http://stm.sciencemag.org/content/11/518/eaaw3680#BIBL
PERMISSIONS	http://www.sciencemag.org/help/reprints-and-permissions